CrystEngComm

Accepted Manuscript

Journal Name

ARTICLE

Emerging Applications of Metal-Organic Frameworks

Raffaele Ricco,[a] Constance Pfeiffer,[b] Kenji Sumida,[c] Christopher J. Sumby,[c] Paolo Falcaro,[a] Shuhei Furukawa,[d] Neil R. Champness[b] and Christian J. Doonan*[c]

Metal-organic Frameworks are a unique class of materials well known for their crystallinity and ultra-high porosity. Since their first report over fifteen years ago, research in this area has sought to actively exploit these properties, especially in gas adsorption. In this article we canvass some emerging topics in the field of MOF research that show promise for new applications in areas such as biotechnology, catalysis, and microelectronics.

Introduction

Metal-organic Frameworks (MOFs) are an established class of porous solids that are known for their chemical mutability and structural flexibility.[1] Since the report of MOF-5 over 15 years ago[2] a significant body of research has focussed on exploring the gas sorption properties of these unique materials.[3,4] Remarkably, MOFs continue to offer rich fundamental insight into the nature of gas adsorption processes[5–7] and demonstrate benchmark storage and separation performance characteristics.[8] Nevertheless, gas sorption can be considered an advanced area of research and has been extensively reviewed.[9–12] In this highlight review we focus on selected emerging applications of MOFs and briefly canvass their potential for further development. Note that our choice of topics is motivated by a number of key publications in the respective areas, and the topic coverage is not intended to be exhaustive in nature. Additionally, several areas of growing interest are omitted, and readers are directed toward other recent review articles.[13–16] Firstly, we will focus on MOFs as novel materials for biotechnology. Then, we highlight studies that establish the potential for using porous crystals as hosts for structural analysis of guest molecules. Finally, we will discuss fundamental developments in the shaping and processing of MOFs as a key to unlock MOF-based device fabrication.

1. MOFs: Towards Novel Biotechnological Applications

The first examples of the application of MOFs in a biological context were as vectors for drug delivery.[17] Given their large pore volumes, structural diversity and tuneable chemical functionality, MOFs represent particularly attractive candidates for drug delivery systems. Work in this area has developed since the first proof-of-principle studies and a greater variety of drugs and MOFs have been explored.[18] A broader scope of applications has also been surveyed, including the use of MOFs as contrast agents for biological imaging and as sensors for biologically relevant molecules.[19–21] In the context of drug delivery, an enhanced fundamental understanding of how the framework stability, pore chemistry and crystal size modulate performance characteristics such as cargo release rates, loading capacities and biocompatibility has ensured significant developments in employing MOFs as drug carriers.[13,22]

Very recently, MOFs have been used to encapsulate biomacromolecules.[23–25] Here, initial efforts addressed the insertion of biological structures into pre-formed MOF, a method pioneered by Lykourinou and coworkers, which post-synthetically infiltrated microperoxidase MP-11[26] and Cytochrome c[27] into Tb-based MOFs. These examples were limited to biomacromolecules with sizes smaller than the MOF cavities, although more recent work by Yaghi and coworkers[28] has demonstrated the precise tuning of the pore size to adsorb and accommodate bigger biomacromolecules, such as myoglobin and green fluorescent protein.

a. Institute of Physical and Theoretical Chemistry, Technical University Graz, Stremayrgasse 9, 8010 Graz, Austria .
b. School of Chemistry, University of Nottingham, University Park, Nottingham NG7 2RD, UK.
c. Department of Chemistry, School of Physical Sciences, The University of Adelaide, North Terrace Campus, Adelaide SA 5005, Australia.
   E-mail: christian.doonan@adelaide.edu.au
d. Institute for Integrated Cell-Material Sciences (WPI-iCeMS), Kyoto University, Yoshida, Sakyo-ku, Kyoto 606-8501, Japan.
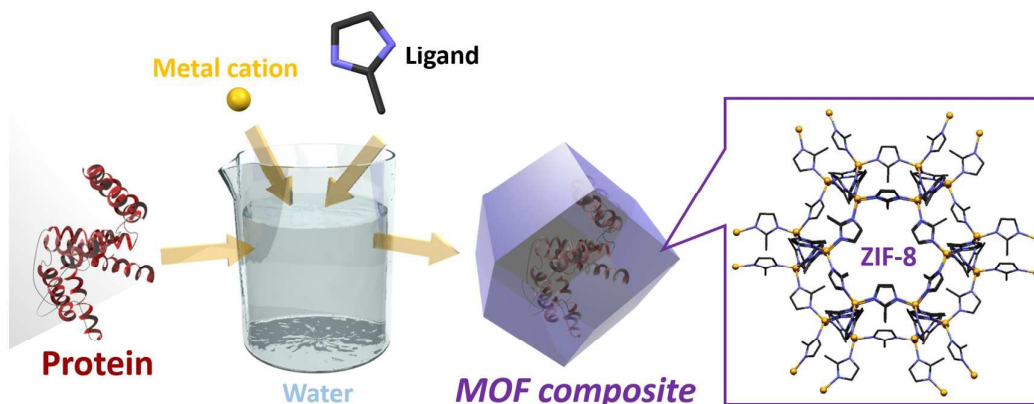
Fig. 1 Schematic describing the preparation of a MOF bio-composite via the biomimetic mineralization process.[25] Protein dissolved in aqueous solution attracts ligand molecules and metal ions, eventually facilitating the nucleation of MOF crystal (ZIF-8 in this example) around the biomacromolecule.

Although the chemistry of MOFs in biological systems has been previously explored, the precipitation of porous frameworks by proteins and enzymes represents a significant advance with potential applications in areas such as biocatalysis and bio-banking. Here, two subtly different methods have been presented for initiating MOF growth around biomacromolecules. In the *co-precipitation* strategy,[23,24] a biocompatible polymer is used as an *in situ* capping agent that presumably acts as a layer between the protein and the MOF. Meanwhile, in the *biomimetic mineralization* approach,[25] the biomacromolecule itself induces MOF crystallization, which mimics the naturally occurring process of biomineralization (**Fig. 1**). A salient feature of both strategies is the ability to embed molecules significantly larger than the MOF pores, whose size usually restricts the diameter of guest molecules that are able to be diffused into the material. This allows for the encapsulation of a vast library of different sized biomacromolecules, and also precludes leaching via pore diffusion. Liang et al. recently reported a comparison of the biomimetic mineralization approach to the co-precipitation method by probing the stability of urease over a variety of temperatures (**Fig. 2a**).[29] In this case the biomimetic mineralization approach outperformed the co-precipitation method in terms of protective capability. This difference is presumably due to the spatial distribution of the enzymes throughout the host framework as the biomimetic approach provides a more homogeneous product with less unprotected, surface-bound guest molecules.[24,29] Interestingly, previous work focusing on the integration of inorganic nanoparticles with MOFs has shown that the spatial localization of poly(vinylpyrrolidone) (PVP) capped nanoparticles in ZIF-8 crystals could be rationally controlled via synthetic conditions.[30] Future investigations may unveil the possibility to position biomacromolecules within the MOF crystals with greater precision, allowing more control over the activity profile and properties of the guest biomolecules.

One of the most promising applications of encapsulated biomolecules within MOFs lies in industrial biocatalysis. A critical first step for demonstrating the viability of such systems requires the MOF coating to provide a protective environment for the enzyme while also allowing the catalytic reaction to readily occur. To this end, Tsung and coworkers have demonstrated that ZIF-90[31] can form a crystalline shell around catalase (CAT), affording a CAT@ZIF-90 composite material (**Fig. 2b**).[23] The protective qualities of the MOF coating were highlighted by successfully carrying-out peroxide decomposition in the presence of proteinase K. In absence of the MOF, catalase loses activity in the presence of the protease, a biomacromolecule used as an enzyme killer agent. However, the rate of H_2O_2 decomposition for CAT@ZIF-90 composite remains unaffected when protease is added to the reaction mixture. This study provided clear evidence that MOFs can be used to introduce species into a single reaction mixture that would normally be incompatible. Indeed, many opportunities exist for extending this idea to combine biocatalysts and inorganic species in one-pot reactions. The concept of enzyme catalysis in a MOF was taken a step further by Liu and co-workers (**Fig. 2c**).[32] In this case, a MOF composite containing two enzymes, glucose oxidase (GOx) and horseradish peroxidase (HRP), was prepared by adding a zinc nitrate solution to a mixture containing the organic linker 2-methylimidazole and both GOx and HRP. To demonstrate the utility of this multi-component system, the authors devised and performed an enzymatic cascade reaction that could selectively sense glucose in solution. Notably, ZIF-8 crystals containing both enzymes significantly outperformed a system where the enzymes were spatially separated by synthesizing distinct bio-composites for each class of enzyme: HRP@ZIF-8 and GOx@ZIF-8. This was attributed to the proximity of the enzymes in the former multi-component system.

MOFs have also recently been explored for the delivery of biologically relevant gases. For example, nitric oxide (NO), known to be a pollutant and toxic gas, was discovered in the late 1980's in endothelium-derived relaxing factor, which is responsible for vasodilation.[33,34] This discovery spurred significant research interests in the context of the chemical and biological effects of NO in the physiological arena. These

studies unveiled the roles of NO as a signalling molecule regulating intercellular communication in not only vasodilation, but also in neurotransmission and immune system responses. Compared to other signalling molecules, NO has several characteristics relying on its unique chemical and physical nature, including high diffusivity, membrane permeability, high reactivity, and short lifetime (< 5s).[35] Currently, researchers have devoted increased attention toward addressing potential therapeutic applications of NO via development of new solid-state materials to deliver exogenous NO in a controlled fashion,[36] However, the precise localization of NO at the single-cell level remains an outstanding challenge.
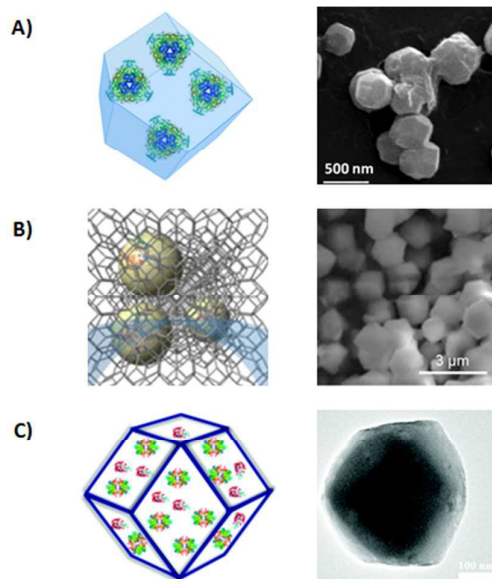
Fig. 2 Representations and corresponding morphological investigations of enzyme@MOF systems prepared by nucleation of MOF around bioactive macromolecules: a) urease@ZIF-8 and SEM image of the obtained particles (Reproduced from Ref. 29 with permission from The Royal Society of Chemistry); b) CAT@ZIF-90 and SEM analysis (Adapted with permission from Ref. 23. Copyright 2015 American Chemical Society); c) (GOx, HRP)@ZIF-8 and TEM characterization of the multi-enzyme MOF composite (Reproduced from Ref. 32 with permission from The Royal Society of Chemistry).

A particular advantage of MOFs over conventional macromolecular scaffolds in NO release applications (e.g. inorganic or silica nanoparticles and organic polymers, is that their comparatively high surface area provides enhanced release efficiencies and greater total NO payloads, both of which are essential for real-world applications. Conventional porous scaffolds, such as zeolites and mesoporous silica, have also been investigated for NO release, and possess certain properties that stem from their unique structural and chemical functionalities. For example, in the area of zeolites, the use of open metal sites to bind NO[37] has been demonstrated. However, the mechanism of their release, which involves a replacement reaction with water molecules, precludes their use under physiological conditions. Meanwhile, the large pores within mesoporous silica have been shown to accommodate large numbers of NO-donor organic molecules via physisorption, resulting in high NO loadings.[38] However, the

encapsulated donor molecules have the propensity to leach out of the pores under physiological conditions due to the lack of chemical anchoring to the material's surface. Metal-organic frameworks (MOFs), which possess an inherent inorganic-organic hybrid nature, provide opportunities to integrate design features derived from both inorganic and organic materials. This may allow the attractive properties of conventional materials to be combined with the high surface areas of MOFs.

In a manner similar to zeolites, the introduction of open metal sites into MOFs has allowed the surface binding of NO by chemisorption, with controlled release via ligand substitution of a water molecule at the metal site. A first example was demonstrated using $Cu_3(btc)_2$ (HKUST-1).[39] Here, the open Cu^{2+} site at the copper paddlewheel units strongly retained one NO molecule per paddlewheel unit (2.21 mmol·g^{-1}) even after the pressure of NO was reduced to almost zero. However, the Cu^{2+}-NO interaction was found to be too strong to allow the release of all of the NO molecules, leading to a very low release efficiency (approximately two orders of magnitude less than the initial loading). To resolve the problem of strong NO binding, or to fine-tune the binding strength, MOFs with isostructural frameworks comprising of different metal ions can be constructed. The $M_2(dobdc)$ series of isoreticular structures (M-CPO-27, M-MOF-74) were tested in NO adsorption and release experiments. Here, $Ni_2(dobdc)$,[40,41] Co(dobdc),[40] Mg(dobdc),[41] Zn(dobdc),[41] and Fe(dobdc),[42] have been studied, revealing that the Ni-, Co-, and Fe-based materials display a strong binding affinity, thereby facilitating a NO occupancy of almost one molecule per open metal site (up to 18 NO molecules per unit cell). Meanwhile, the Mg- and Zn-based frameworks showed significantly lower loading efficiencies: uptakes of ten and five NO molecules per unit cell for the Zn- and Mg-based analogues, respectively. Furthermore, the metal ions were also found to strongly influence the release kinetics. The Ni- and Co-based frameworks released the majority of adsorbed NO molecules within a few hours under 11% relative humidity, while the Fe-based compound showed strong binding with a concomitantly slow release of two-thirds of the molecules over a duration of ten days. Compared to these three compounds, the Zn- and Mg-based frameworks released very low amounts of NO (0.5 and 0.08 NO molecules per unit cell, respectively), although the doping of Ni^{2+} ions into these frameworks significantly enhanced the storage capacity and releasing efficiency, allowing performance to be tuned systematically.[43]

Besides fine-tuning NO binding strength through the formation of isostructural frameworks, another advantage of MOFs is the designability of organic linkers, which allows the introduction of NO-containing moieties into the framework scaffolds. For example, the diazeniumdiolate functionality (also commonly referred to as NONOate), was introduced into MOF scaffolds for controlled release of NO by moisture.[44,45]

While all of the MOF-based systems described above released NO molecules via displacement or reaction with water molecules, alternative triggering methods are essential when considering the usage of these compounds under

physiological conditions. This can be achieved by designing an organic linker to release NO through different mechanisms. One of the alternative approaches is to use light as a trigger to release NO because this allows spatial and temporal control over the release process. Nitroaromatic compounds are known to be photoactive NO-donors, and nitroimidazole groups have been incorporated in a zeolitic imidazolate framework (ZIF), $Zn(2nIm)_2$ (NOF-1) and $Zn(mnIm)_2$ (NOF-2) (NOF = nitric oxide framework, 2nIm = 2-nitroimidazole and mnIm = 5-methyl-4-(Error! Reference source not found.).[46] These frameworks did not release any NO molecules under ambient conditions, but did release NO under UV light irradiation. NO release duration and kinetics could be controlled by the irradiation time and intensity, respectively. Note that pure samples of the ligands, 2nIm and mnIm, did not release NO molecules even under the light irradiation due to an intermolecular quenching process. The photoactive release of NOF-1 and NOF-2 reached 50% and 46%, respectively, with a total release amount of 3.4 and 2.9 mmol·g^{-1}, which are the highest among the light-triggered NO-releasing macromolecule scaffolds.

Fig. 3 Spatiotemporally controlled release of NO. (A) Schematic illustration of the localized cell-stimulation platform based on NOF-1 crystals. The generated NO by two-photon near-infrared laser irradiation diffuses through the PDMS layer and reacts with an intracellular NO fluorescent indicator, DAF-FM. (B) Confocal microscopy images of NOF-1-embedded substrates cultured with HEK293 cells introduced via DAF-FM. The localized photoactivation of the NOF-1 crystals (white squares) induced a fluorescent response in the surrounding cells (scale bar, 100 mm). Further demonstration of spatiotemporal control by writing 'N', 'O', 'F' upon activation of the selected regions (scale bar, 100 mm). (Adapted with permission from Ref. 46. Copyright Nature Publishing Group).

Another reaction mechanism using the bis-N-nitrosoamine moiety was introduced into the stable MOFs with high valent metal ions, $Ti_8O_8(OH)_4(MeNNO-bdc)_6$ (NOF-11) and $Al_8(OMe)_8(OH)_4(MeNNO-bdc)_6$ (NOF-12), which display the MIL-125 and CAU-1 structure types, respectively (MeNNO-bdc = 2,5-bis(methyl (nitroso) amino)-1,4-benzene-dicarboxylate).[47] Both frameworks release NO with high photoactive efficiencies (40% and 58% for NOF-11 and -12, respectively). Importantly, the higher charge of the Ti^{4+} cation compared to Al^{3+} provides stronger metal-ligand bonding and an enhanced stability profile for NOF-11 compared to NOF-12 in both water and in buffer solutions. Overall, the manipulation of both the inorganic and organic components of MOFs has provided new developments for cell biology applications, and in vivo studies have recently emerged. Further efforts in developing physiologically-stable MOFs with a controlled NO-releasing property would certainly contribute to new insights in the biological importance of NO, and the development of potential therapies employing gas molecules.

2. MOF as Crystallisation Matrices

The periodic structure of MOFs and their ability to selectively adsorb certain guest molecules[48–52] has led to their investigation as matrices for hosting guest molecules in an ordered, structurally-definite fashion. In a recent extension to their use of porous cage structures in solution, Fujita and co-workers have developed an approach that employs a MOF (which they term a 'crystal sponge') that can be used to trap guests in a periodic arrangement, thereby facilitating their direct, X-ray crystallographic structural determination.[53] More specifically, the $[(Co(NCS)_2)_3(2,4,6-tris(4-pyridyl)-1,3,5-triazine)_4]$.x(solvent) and $[(ZnI_2)_3(2,4,6-tris(4-pyridyl)-1,3,5-triazine)_2]$.x(solvent) compounds were shown to act as compatible hosts for a variety of guest molecules,[53,54] allowing nanogram quantities of unknown compounds to be structurally characterized by single crystal X-ray diffraction (SCXRD). In principle, the approach obviates the need to separately crystallize the target molecule, and permits structural analysis even in instances where only small quantities are available. The generalized use of the 'crystalline sponge' strategy still remains challenging, and critically requires a versatile host framework to be able to adsorb a wide range of guest molecules in a highly ordered fashion. However, the potential to inspect unstable moieties or molecules that are not easily crystallised in pure form is highly attractive, and a range of targets has been recently investigated to further demonstrate the utility of the strategy.[54–61] The characterised guest molecules range from simple molecules[54] to reactive acrylate esters[56] and complex

Journal Name

ARTICLE

molecules with axial and planar chirality,[58] (1R)-(—)-menthyl acetate,[59] α-humulene and its oxidized subproducts.[60] The 'crystalline sponge' approach has also been developed for porous organic materials[61] mirroring studies in MOFs.

In addition to the 'crystalline sponge' approach, post-synthetic encapsulation of molecules within pore voids, wherein the molecular architecture of frameworks is utilized to lock functionalized molecules (so-called cartridges) between the pore walls, has been successfully employed for structural characterization. In a landmark study, a Schiff-base reaction was probed allowing the direct structural characterisation of an intermediate hemiaminal group,[55] which had remained elusive via conventional structural characterization techniques (**Fig. 4**). Here, a MOF formed from the reaction of ZnI_2 and 2,4,6-tris(4-pyridyl)-1,3,5-triazine was used to trap an electron-rich 1-aminotriphenylene cartridge, which was found to occupy a position between the electron deficient layers formed by the 2,4,6-tris(4-pyridyl)-1,3,5-triazine ligands of the host framework. Close examination of the structure revealed that the amine group of the trapped cartridges pointed into the pore channels, and its reactivity in the solid-state was subsequently probed. A condensation reaction with acetaldehyde was successfully carried out in a single-crystal to single-crystal process, and analysis of the diffraction data showed that at low temperatures a hemiaminal species could be kinetically trapped and structurally characterised, highlighting the power of the technique.
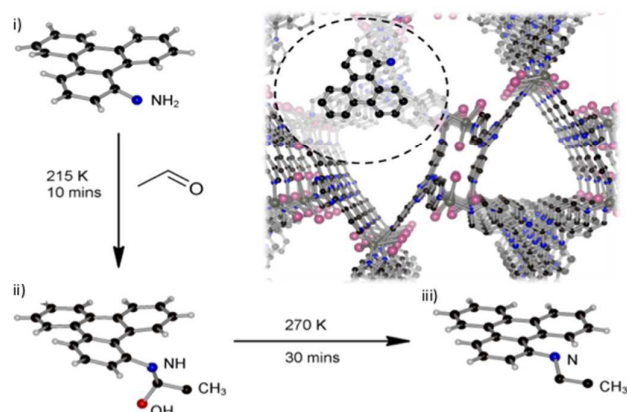
Fig. 4 i) 1-aminotriphenylene guest molecule is hosted by the $\{[ZnI_2)_3(2,4,6\text{-tris}(4\text{-pyridyl})\text{-}1,3,5\text{-triazine})_2]N_x(\text{solvent})\}_n$ framework, sitting between 2,4,6-tris(4-pyridyl)-1,3,5-triazine ligands; ii) subsequent reaction with acetaldehyde leads to the isolation of a transient hemiaminal intermediate, formed within the MOF pores; iii) subsequent heating leads to formation of the final imine product. (Reproduced with permission from Ref. 62. Copyright 2015 WILEY-VCH Verlag GmbH %26 Co. KGaA, Weinheim).

In an elegant extension to these approaches, time-dependent X-ray crystallography has been employed to evaluate a reaction involving Pd-mediated bromination of a phenyl group.[57] Here, the MOF environment provides a rigid matrix upon which the chemical transformations through a Ar−Pd−Br intermediate and the subsequent elimination of the Pd atom to the brominated, Ar−Br, product can be identified through close inspection of electron density maps. The observation of a Pd^{2+} intermediate is an important feature of

this work because in solution such compounds typically rapidly convert to dinuclear $Pd_2(\mu\text{-Br})_2$ species and are precipitated from solution. In contrast, the MOF-embedded structure prohibits the dimerization process, allowing identification of the intermediate Ar−Pd−Br species. One caveat to this approach is that the observed intermediate is formed within the unique environment of the MOF, which may place constraints on the complex geometry and affect the potential reaction pathways and the structure of the observed intermediate species.

In addition to the examples above, wherein the guest molecules are accommodated within the pores via an adsorption-based pathway, one further approach for the identification and characterisation of intermediates in chemical reactions involves the direct grafting of a target molecule to the framework itself. The strategy employs appropriately designed organic struts that not only bridge structural metal centres but also provide coordination sites to bind the metal complexes for subsequent investigation. In this manner the target complex is anchored to the MOF scaffold rather than being a structural component required for framework assembly. An important consequence of this approach is that the target of investigation can be modified (converted to other species of interest) without disrupting the framework structure.[63] Thus, it is more likely that chemical transformations of the target will not interfere with the overall crystallinity of the MOF. The preservation of the single-crystallinity of the sample consequently facilitates the characterisation of any chemical transformation (e.g. by photochemical conversion) of the supported target species via X-ray diffraction studies.
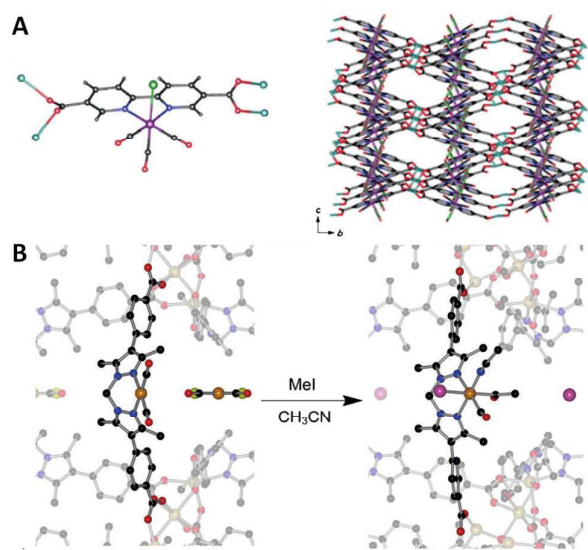
Fig. 5 (A) View of the $\{M(2,2'\text{-bipyridine-5,5'-dicarboxylate})(CO)_3X\}$ (M = Re, Mn, X = Cl, Br) ligand that is used to create a complex-bearing MOF through reaction of the carboxylate groups with Mn^{2+} salts. (B) The oxidative addition of MeI to a $[Rh(CO)_2]^+$ complex within the pores of $\{Mn_3(L)_2(L')\}n$. X-ray structures of (left) $\{Mn_3(L)_2[(Rh(L')(CO)2][RhCl_2(CO)_2]\}_n$ and (right) $\{Mn_3(L)_2[Rh(L')(CO)(NCMe)(COMe)I]I\}_n$ [L = bis(4-(4-carboxyphenyl)-1H-3,5-dimethylpyrazolyl)methane]. (Reproduced with permission from (A) Ref 64 and (B) Ref 65. Copyright Nature Publishing Group).
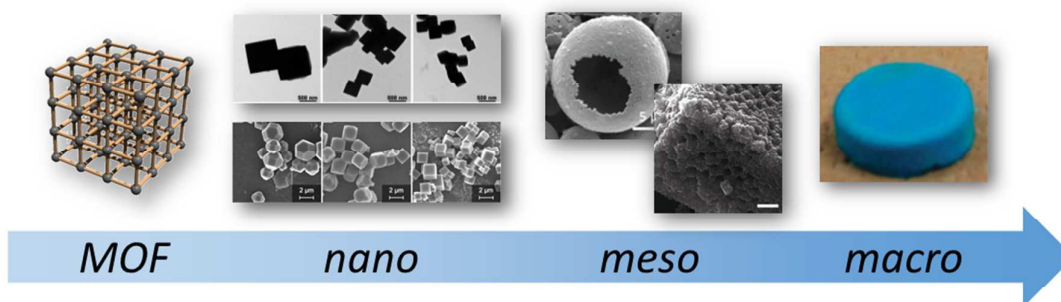
Fig. 6. Examples of structuralisation of MOFs at the nanoscale, through modulation of the crystal size and morphology, at the mesoscale, by manipulating mutual intergrowth or epitaxial growth of the crystals to form larger assemblies, and finally at the macroscale by controlling the internal organisation of the solid and overall external shaping to match the specifications required for the application.

The incorporation of a target metal complex within the pores of a MOF has been successfully achieved via grafting of the moiety to non-structural anchoring points both before (pre-synthetic modification) and after (post-synthetic modification) the assembly of the MOF.[62] An example of pre-synthetic incorporation of a target complex for subsequent investigation is the use of the M(2,2'-bipyridine-5,5'-dicarboxylate)(CO)$_3$X (M = Re, Mn; X = Cl, Br) as a ligand in the construction of MOFs, with the carboxylate donors of the carboxylate functionalities binding either Mn^{2+} or Cu^{2+} during framework formation.[64,66] The M(diimine)(CO)$_3$X unit is supported by the framework, sitting upon one of the struts of the MOF and does not act to propagate the MOF structure (**Fig. 5Error! Reference source not found.a**). The M(diimine)(CO)$_3$X moiety, whether Re or Mn, has well-understood photochemistry which can be probed by time-resolved spectroscopic studies, notably picosecond time-resolved IR (TRIR), allowing an understanding of the effect of the MOF environment on the properties of the framework-supported complex. TRIR studies of the MOF-supported Re(diimine)(CO)$_3$Cl complex confirm the formation of both 3MLCT and 3IL (intra-ligand) π-π* states. However, the MLCT bands decay rapidly (ca. 20 ps), concurrent with further growth of the intra-ligand 3π-π* transition. Further, the TRIR spectra obtained 1 ns after excitation reveal the presence of only the intra-ligand 3π-π* states. The 3π-π* state of Re(2,2'-bipy)(CO)$_3$Cl is not normally accessible in solution due to its higher energy than the commonly observed 3MLCT state, and it can be concluded that the MOF environment directly affects the nature and relative stabilities of the excited states of the framework-supported complex. Under suitable conditions it is possible to isomerise the M(diimine)(CO)$_3$X moiety and this has been demonstrated for the MOF that contains the Mn(2,2'-bipyridine-5,5'-dicarboxylate)(CO)$_3$X (X = Cl, Br) framework strut, Mn(DMF)$_2$[(2,2'-bipy'-5,5'-dicarboxylate)Mn(CO)$_3$X]. Irradiation of this Mn-containing MOF results in 25% fac-to-mer isomerisation, allowing direct characterisation of the isomerisation product by SCXRD experiments.[64] The use SCXRD as a powerful tool to probe reaction chemistry in MOFs has been further demonstrated in metalated porphyrin-containing MOFs.[67] The study uses PCN-224, a Zr-based MOF that uses tetracarboxyphenylporphyrin bridging ligands. The MOF can be post-synthetically metalated to introduce Fe^{2+} cations to the porphyrin core, and the metalated MOF reacts with gaseous O$_2$ at 195 K, mimicking heme-like reactivity. The process can be followed by SCXRD, establishing the structure of the heme-O$_2$ complex, which represents the first structurally-characterized example of a five-coordinate heme-O$_2$ adduct. This result further demonstrates that MOFs are capable of stabilising unusual chemical species that are only observed transiently in its molecular form.

Similarly, post-synthetic modification of MOFs can be used to introduce metal complexes to the vacant coordination site on the MOF linkers. Although post-synthetic metalation has been demonstrated for a range of MOFs, most materials fail to retain their single-crystallinity following the metal insertion process.[63] However, the Mn^{2+}-based framework Mn$_3$L$_3$ (Mn-MOF-1; L = bis((4-(4-carboxyphenyl)-1H-3,5-dimethylpyrazolyl)methane), whose ligand backbone incorporates a vacant bispyrazolate binding site.[67] Post-synthetic metalation can be employed to insert a range of metal complexes into the structure, and has been successfully employed in binding a range of metal salts including CoCl$_2$, CuCl$_2$, Zn(NO$_3$)$_2$, and Cd(NO$_3$)$_2$.[65,68] A simple example that demonstrates the power of the technique is demonstrated by the post-synthetic metalation using CoCl$_2$.6H$_2$O to generate the [Mn$_3$L$_3$]Co(H$_2$O)$_4$·2Cl. Upon heating, the crystals were found to change colour from pink to blue, with removal of the water ligands on the Co^{2+} metal centre and substitution with two chloride ligands to give the [Mn$_3$(L)$_3$]CoCl$_2$ compound. The colour change is rationalised by the change in geometry from octahedral to tetrahedral, a change which could be directly observed by SCXRD. Interestingly, in addition to the change in geometry and coordination environment of the Co^{2+} centre, a significant rotation about the central carbon atom of the linker (which acts like a 'hinge') is observed, highlighting the importance of the flexibility of the MOF in accommodating a variety of coordination environments, as well as the preservation of the single-crystal nature of the samples.

The potential scope of the post-synthetic metalation strategy was further demonstrated by the introduction of $[Rh(CO)_2Cl]_2$ into the Mn_3L_3 framework, which proceeds in essentially quantitative yield to afford the $[Mn_3L_3]Rh(CO)_2 \cdot RhCl_2(CO)_2$ species (**Fig. 5Error! Reference source not found.b**).[65] Following metalation, two Rh(I) centres are present in the framework: a $[Rh(CO)_2]$ moiety bound to the bispyrazolate site, and a $[RhCl_2(CO)_2]^-$ counter-anion which lies within the MOF pores. Exposure of the framework to methyl iodide results in oxidative addition at the framework-bound metal centre, and the process could be directly probed by SCXRD. Indeed, the crystallographic data unambiguously demonstrate the oxidative addition reaction and show the formation of a bis-pyrazolate bound $[Rh(CO)(NCMe)(COMe)I]I$ species. Here, the Rh^{3+} metal centre adopts an octahedral geometry, with the CO and MeCN ligands in the equatorial plane and the iodide and the C(=O)Me ligands occupying the axial positions. In this case, the SCXRD experiments unambiguously allow the conformation of the ligands about the metal centre to be determined, which presents a difficult challenge via conventional spectroscopic methods for porous solids.

3. Structuring of Metal-Organic Frameworks

The successful integration of MOFs as a functional component of real-world systems requires precise control over and optimisation of the physical form of the material across all length scales.[69] This involves considerations that are independent of the composition of the material (i.e. the identity of the metal and organic linker), and includes modulation of the crystal size and morphology (nanoscale), mutual intergrowth or epitaxial growth of the crystals to form larger assemblies (mesoscale), and finally the internal organisation of the solid and overall external shaping to match the specifications required for the specific application (macroscale) (**Fig. 6**). Here, the bottom-up synthetic methods used in the context of other inorganic and hybrid materials, including sol-gel processing, flow chemistry and microfluidics, and surface functionalisation techniques, have inspired new strategies for the preparation of structuralised MOF-based materials with enhanced properties compared to their bulk (powder) counterparts.[70–72]
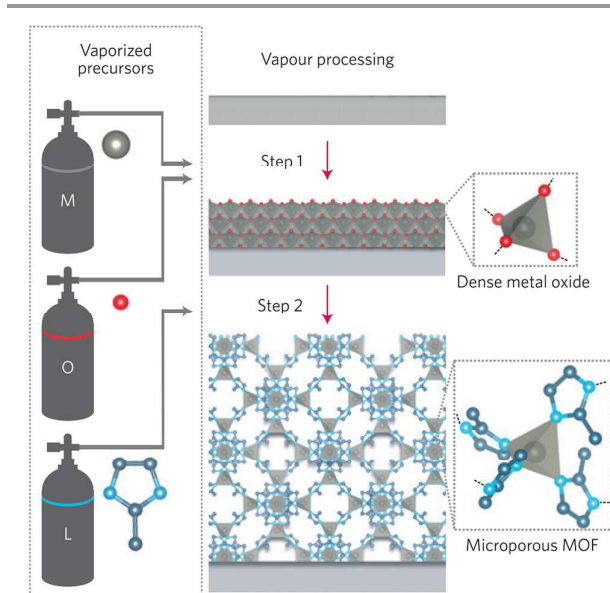
Fig. 7 Chemical vapour deposition of thin film MOF coatings via a two-step process involving the preliminary deposition of a metal oxide coating (step 1) followed by a ligand mediated conversion to a microporous MOF (Reproduced with permission from Ref. 73. Copyright Nature Publishing Group)

The manipulation of the crystal size and shape of MOFs in the nanometre regime is crucial in order to enhance diffusion rates[74] and compatibility with support materials when integrated in composite systems.[75,76] In some structure types, new material properties can also emerge within certain crystal size domains. For example, downsizing of crystals of the elastically flexible $Cu_2(bdc)_2(bpy)$ framework to ca. 50 nm is found to introduce a third, metastable structural phase (a 'guest-free open' phase) that cannot be accessed in larger crystals of the same compound.[77] Similarly, the sorption properties and flexibility of the ZIF-8 framework are significantly influenced by the crystal size.[78] In this case, the pressure at which the guest-induced structural transition occurs (resulting in a step in the N_2 isotherm at 77 K) increased as the size of the crystals was reduced. In both cases, the downsizing of the crystals suppresses the structural mobility of the framework, although it is not yet known if this is a phenomenon common to all flexible frameworks.

Commonly, strategies to control particle size or shape are implemented during synthesis but an alternative, post-synthetic mechanism to shaped and size-controlled particles was recently reported by Imaz and Maspoch, and relies on controllably etching micron or mesoscale crystals.[79] In addition to avoiding the need to perturb carefully refined synthetic conditions, notably, this method may give access to morphologies not available from the synthetic approaches utilised elsewhere.

At the mesoscale, the organisation of MOF crystals into hollow, capsule-like structures composed of a nanoporous shell offer considerable potential in chemical catalysis[80] and biomedical applications.[22] This structure provides an encapsulated space that is separated from the exterior

environment of the capsule, yet which is still accessible to small molecules as a consequence of the nanoporous nature of the shell. These structures offer significant potential as catalysts, since catalytic nanoparticles can be enclosed within the hollow structure (in so-called 'yolk-shell' materials), while the MOF-based shell facilitates selective molecular diffusion into and out of the architecture. In a recent example, an agarose hydrogel droplet Pickering-stabilised by UiO-66 and magnetite nanoparticles was used as a template for ZIF-8 growth.[81] The hydrogel core permits the storage of biomolecules, such as enzymes, within the capsules as a biocatalyst. Furthermore, they are found to be highly robust and readily collected by a magnet, allowing the material to be recycled following use.

Recently, some additional synthetic developments have further broadened the scope for structuralising at the mesoscale. In particular, Falcaro and Kim reported microfluidic approaches to functional bio-MOF hollow spheres with precisely controlled size regimes in a continuous manner,[82] while Kitagawa and co-workers utilised a process similar to the Kirkendall effect[83] to transform a solid MOF crystal into a hollow structure.[84] Eddaoudi's group has also demonstrated that emulsion-based techniques can be elegantly used to induce the self-assembly of non-spherical building blocks into 3D hollow MOF superstructures.[85]

The deposition of microporous MOFs as coatings or thin-films on metal or oxide surfaces is attractive for synergistically combining the porous properties of the framework with those of the support. Here, the layer-by-layer method is a convenient method that facilitates growth of the MOF layer with a precise thickness via the frequency of precursor cycling employed during the growth step. This strategy has recently

been demonstrated for the preparation of heterostructured films, allowing growth of films comprising multiple frameworks to be deposited in a core-shell fashion, with control over the thickness of each individual MOF component.[86] In one recent example, the secondary growth of a small pore $Zn_4O(3\text{-methyl-}5\text{-isopropyl-4-carboxypyrazolate})_3$ framework upon a larger-pore $Zn_4O(3,5\text{-dimethyl-carboxypyrazolate})_3$ film deposited on a quartz crystal microbalance (QCM) substrate resulted in a film exhibiting a high size-selectivity toward the adsorption of alcohol molecules.

A breakthrough in synthetic approaches to realise thin film coatings for microelectronics was recently described by Ameloot and co-workers.[73] They used a chemical vapour deposition process to prepare high-quality films of ZIF-8, with a uniform and controlled thickness (**Fig. 7**). This approach relies upon a preliminary deposition of a dense metal oxide coating that can be processed into a microporous MOF (ZIF-8) with the introduction of the ligand (2-methylimidazole). Importantly, this synthetic advance translates MOF thin film fabrication approaches closer to those used in microelectronics research and for industry.[73] Patterning of MOF coatings is also a strongly emerging direction in MOF chemistry with interest in microfluidic and sensing devices being paramount. Among recent approaches to pattern MOF coatings, examples include the use of ZnO particles[87] and even biomolecules.[88]

The structuring of MOFs into meso- and macrostructured materials has also been addressed recently via the direct conversion of inorganic materials by the so-called 'coordination replication' technique. Following an initial demonstration of the conversion of alumina substrates into Al-based frameworks,[89] the scope of the technique has since
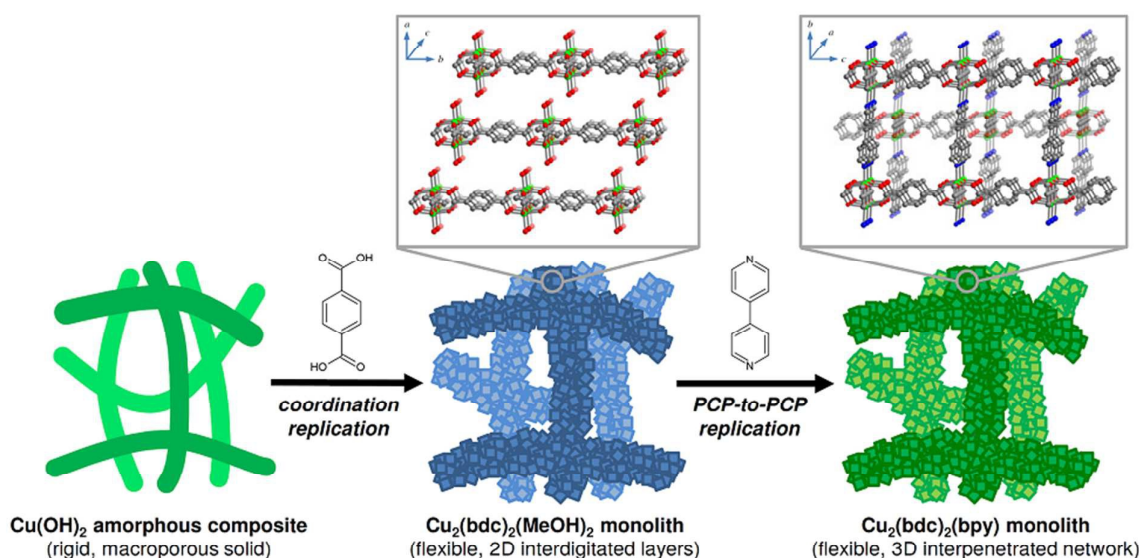
Fig. 8. A schematic showing the structuring of MOFs via replication of a sol-gel derived Cu(OH)₂-polyacylamide amorphous composite firstly into a monolith composed of the two-dimensional $Cu_2(bdc)_2(MeOH)_2$ framework, followed by pillaring of the layers to form the corresponding structure of the flexible $Cu_2(bdc)_2(bpy)$ framework (Reproduced from Ref. 93 with permission from The Royal Society of Chemistry).

been extended to other metals, including non-oxide precursors.[90,91] In a recent report, a macroporous copper hydroxide-polyacrylamide (PAAm) monolithic precursor could be converted to the corresponding structuralised form of HKUST-1.[92] Here, the rapid conversion rate (< 5 min under mild solvothermal conditions) facilitated the conversion of centimetre-sized monoliths, with retention of the original macroporosity and concomitant introduction of microporosity originating from the MOF phase. Meanwhile, the conversion of the same precursor to the flexible frameworks $Cu_2(bdc)_2(MeOH)_2$ and $Cu_2(bdc)_2(bpy)$[93] (**Fig. 8**) revealed an influence of the polymer phase and physical immobilisation of the crystals on the dynamic properties of the frameworks when compared to the bulk materials. Establishing a greater understanding of such factors is expected to play an important role in the successful integration and optimisation of MOFs within higher-order structures. In one approach to overcoming the challenges of integration and loading of MOF particles into composite materials, Cohen and co-workers have developed polyMOFs,[94] hybrid materials in which the MOF 'additive' and the polymer 'support' are chemically integrated. Such systems were initially reported with MOF-5 analogues but have been extended to photo-linked UiO-66 composites[95] and used to produce high MOF-loading mixed matrix membrane composite materials.[96]

Future Directions

It is evident that the chemistry of metal-organic frameworks is rapidly expanding into diverse areas that make full use of their 'programmable' structures and chemistry. Correspondingly there is an increasing focus on the chemistry of the MOF structure itself and how it can be modified rather than the 'space' available within the pores. A notable aspect of the emerging areas highlighted in this review is that they are high value applications that require small scale material production relative to industrial catalysis or gas storage and separation systems. This allows for exploration of bespoke materials constructed from non-commercially available organic units as performance characteristics are of key importance. Accordingly, it can be anticipated that such applications will increasingly drive MOF research towards the fields of biotechnology, microelectronics and advanced composites. Indeed the fundamental research described in this review paves the way for these exciting new applied developments.

Additionally, the bespoke crystallisation support materials described offer considerable opportunity in research to elucidate novel reaction chemistry, structurally characterise unstable species or allow effective time-resolved X-ray crystallography of multi-component reactions. Finally, care and attention to structuralisation has led to numerous fundamental discoveries in MOF chemistry, including very recent observations that showed that simply downsizing a rigid, non-porous MOF to a thin film endows it with dynamic, gate-opening-type guest uptake behaviour.[97] Thus, MOFs traditionally considered rigid may be induced to take on dynamic properties with careful control over their structuralisation. Furthermore, the development of photonic MOF-based systems also requires precise control of structuralisation. For example, hybrid photonic films formed by deposition of MOF layers onto 3D ordered colloidal crystal arrays,[98] 1D photonic crystals embedded with micro- and mesoporosity,[99] photonic MOF multilayers,[100] and flexible MOF based 1D photonic crystals fabricated by spin-coating.[101]

References

1   H. Furukawa, K. E. Cordova, M. O'Keeffe and O. M. Yaghi, *Science*, 2013, **341**, 1230444.
2   H. Li, M. Eddaoudi, M. O'Keeffe and O. M. Yaghi, *Nature*, 1999, **402**, 276–279.
3   K. Sumida, D. L. Rogow, J. A. Mason, T. M. McDonald, E. D. Bloch, Z. R. Herm, T.-H. Bae and J. R. Long, *Chem. Rev.*, 2012, **112**, 724–781.
4   M. P. Suh, H. J. Park, T. K. Prasad and D.-W. Lim, *Chem. Rev.*, 2012, **112**, 782–835.
5   R. B. Getman, Y.-S. Bae, C. E. Wilmer and R. Q. Snurr, *Chem. Rev.*, 2012, **112**, 703–723.
6   H. Sung Cho, H. Deng, K. Miyasaka, Z. Dong, M. Cho, A. V. Neimark, J. Ku Kang, O. M. Yaghi and O. Terasaki, *Nature*, 2015, **527**, 503–507.
7   J. A. Mason, J. Oktawiec, M. K. Taylor, M. R. Hudson, J. Rodriguez, J. E. Bachman, M. I. Gonzalez, A. Cervellino, A. Guagliardi, C. M. Brown, P. L. Llewellyn, N. Masciocchi and J. R. Long, *Nature*, 2015, **527**, 357–361.
8   J.-R. Li, J. Sculley and H.-C. Zhou, *Chem. Rev.*, 2012, **112**, 869–932.
9   J. Liu, P. K. Thallapally, B. P. McGrail, D. R. Brown and J. Liu, *Chem. Soc. Rev.*, 2012, **41**, 2308–2322.
10 D. J. Collins and H.-C. Zhou, *J. Mater. Chem.*, 2007, **17**, 3154–3160.
11 L. J. Murray, M. Dincă and J. R. Long, *Chem. Soc. Rev.*, 2009, **38**, 1294–1314.
12 H. Wu, Q. Gong, D. H. Olson and J. Li, *Chem. Rev.*, 2012, **112**, 836–868.
13 P. Horcajada, R. Gref, T. Baati, P. K. Allan, G. Maurin, P. Couvreur, G. Férey, R. E. Morris and C. Serre, *Chem. Rev.*, 2012, **112**, 1232–1268.
14 L. E. Kreno, K. Leong, O. K. Farha, M. Allendorf, R. P. Van Duyne and J. T. Hupp, *Chem. Rev.*, 2012, **112**, 1105–1125.
15 J.-L. Wang, C. Wang and W. Lin, *ACS Catal.*, 2012, **2**, 2630–2640.
16 M. Yoon, R. Srirambalaji and K. Kim, *Chem. Rev.*, 2012, **112**, 1196–231.
17 P. Horcajada, C. Serre, M. Vallet-Regí, M. Sebban, F. Taulelle and G. Férey, *Angew. Chem. Int. Ed.*, 2006, **45**, 5974–5978.
18 A. C. McKinlay, R. E. Morris, P. Horcajada, G. Férey, R. Gref, P. Couvreur and C. Serre, *Angew. Chem. Int. Ed.*, 2010, **49**, 6260–6266.
19 I. Imaz, M. Rubio-Martínez, J. An, I. Solé-Font, N. L. Rosi and D. Maspoch, *Chem. Commun.*, 2011, **47**, 7287.
20 J. Della Rocca and W. Lin, *Eur. J. Inorg. Chem.*, 2010, 3725–3734.

21 J. Lei, R. Qian, P. Ling, L. Cui and H. Ju, *TrAC Trends Anal. Chem.*, 2014, **58**, 71–78.

22 M. Giménez-Marqués, T. Hidalgo, C. Serre and P. Horcajada, *Coord. Chem. Rev.*, 2016, **307**, 342–360.

23 F.-K. Shieh, S.-C. Wang, C.-I. Yen, C.-C. Wu, S. Dutta, L.-Y. Chou, J. V. Morabito, P. Hu, M.-H. Hsu, K. C.-W. Wu and C.-K. Tsung, *J. Am. Chem. Soc.*, 2015, **137**, 4276–4279.

24 F. Lyu, Y. Zhang, R. N. Zare, J. Ge and Z. Liu, *Nano Lett.*, 2014, **14**, 5761–5765.

25 K. Liang, R. Ricco, C. M. Doherty, M. J. Styles, S. Bell, N. Kirby, S. Mudie, D. Haylock, A. J. Hill, C. J. Doonan and P. Falcaro, *Nat. Commun.*, 2015, **6**, 7240.

26 V. Lykourinou, Y. Chen, X.-S. Wang, L. Meng, T. Hoang, L.-J. Ming, R. L. Musselman and S. Ma, *J. Am. Chem. Soc.*, 2011, **133**, 10382–10385.

27 Y. Chen, V. Lykourinou, C. Vetromile, T. Hoang, L.-J. Ming, R. W. Larsen and S. Ma, *J. Am. Chem. Soc.*, 2012, **134**, 13188–13191.

28 H. Deng, S. Grunder, K. E. Cordova, C. Valente, H. Furukawa, M. Hmadeh, F. Gándara, A. C. Whalley, Z. Liu, S. Asahina, H. Kazumori, M. O'Keeffe, O. Terasaki, J. F. Stoddart and O. M. Yaghi, *Science*, 2012, **336**, 1018–23.

29 K. Liang, C. J. Coghlan, S. G. Bell, C. Doonan and P. Falcaro, *Chem. Commun.*, 2015, **52**, 473–476.

30 G. Lu, S. Li, Z. Guo, O. K. Farha, B. G. Hauser, X. Qi, Y. Wang, X. Wang, S. Han, X. Liu, J. S. DuChene, H. Zhang, Q. Zhang, X. Chen, J. Ma, S. C. J. Loo, W. D. Wei, Y. Yang, J. T. Hupp and F. Huo, *Nat. Chem.*, 2012, **4**, 310–316.

31 W. Morris, C. J. Doonan, H. Furukawa, R. Banerjee and O. M. Yaghi, *J. Am. Chem. Soc.*, 2008, **130**, 12626–12627.

32 X. Wu, J. Ge, C. Yang, M. Hou and Z. Liu, *Chem. Commun.*, 2015, **51**, 13408–13411.

33 L. J. Ignarro, R. E. Byrns, G. M. Buga and K. S. Wood, *Circ. Res.*, 1987, **61**, 866–879.

34 R. M. J. Palmer, A. G. Ferrige and S. Moncada, *Nature*, 1987, **327**, 524–526.

35 B. E. Mann and R. Motterlini, *Chem. Commun.*, 2007, 4197–4208.

36 D. A. Riccio and M. H. Schoenfisch, *Chem. Soc. Rev.*, 2012, **41**, 3731–3741.

37 P. S. Wheatley, A. R. Butler, M. S. Crane, S. Fox, B. Xiao, A. G. Rossi, I. L. Megson and R. E. Morris, *J. Am. Chem. Soc.*, 2006, **128**, 502–509.

38 B. J. Heilman, J. St. John, S. R. J. Oliver and P. K. Mascharak, *J. Am. Chem. Soc.*, 2012, **134**, 11573–11582.

39 B. Xiao, P. S. Wheatley, X. Zhao, A. J. Fletcher, S. Fox, A. G. Rossi, I. L. Megson, S. Bordiga, L. Regli, K. M. Thomas and R. E. Morris, *J. Am. Chem. Soc.*, 2007, **129**, 1203–1209.

40 A. C. McKinlay, B. Xiao, D. S. Wragg, P. S. Wheatley, I. L. Megson and R. E. Morris, *J. Am. Chem. Soc.*, 2008, **130**, 10440–10444.

41 D. Cattaneo, S. J. Warrender, M. J. Duncan, R. Castledine, N. Parkinson, I. Haley and R. E. Morris, *Dalton Trans*, 2016, **45**, 618–629.

42 E. D. Bloch, W. L. Queen, S. Chavan, P. S. Wheatley, J. M. Zadrozny, R. Morris, C. M. Brown, C. Lamberti, S. Bordiga and J. R. Long, *J. Am. Chem. Soc.*, 2015, **137**, 3466–3469.

43 D. Cattaneo, S. J. Warrender, M. J. Duncan, C. J. Kelsall, M. K. Doherty, P. D. Whitfield, I. L. Megson and R. E. Morris, *RSC Adv.*, 2016, **6**, 14059–14067.

44 M. J. Ingleson, R. Heck, J. A. Gould and M. J. Rosseinsky, *Inorg. Chem.*, 2009, **48**, 9986–9988.

45 J. G. Nguyen, K. K. Tanabe and S. M. Cohen, *CrystEngComm*, 2010, **12**, 2335–2338.

46 S. Diring, D. O. Wang, C. Kim, M. Kondo, Y. Chen, S. Kitagawa, K. Kamei and S. Furukawa, *Nat. Commun.*, 2013, **4**, 2684.

47 C. Kim, S. Diring, S. Furukawa and S. Kitagawa, *Dalton Trans.*, 2015, **44**, 15324–15333.

48 Y. Inokuma, T. Arai and M. Fujita, *Nat. Chem.*, 2010, **2**, 780–3.

49 S.-Y. Zhang, L. Wojtas and M. J. Zaworotko, *J. Am. Chem. Soc.*, 2015, **137**, 12045–9.

50 Y. Peng, T. Gong, K. Zhang, X. Lin, Y. Liu, J. Jiang and Y. Cui, *Nat. Commun.*, 2014, **5**, 4406.

51 R. E. Morris and X. Bu, *Nat. Chem.*, 2010, **2**, 353–61.

52 L. Ma, C. Abney and W. Lin, *Chem. Soc. Rev.*, 2009, **38**, 1248–56.

53 Y. Inokuma, S. Yoshioka, J. Ariyoshi, T. Arai, Y. Hitora, K. Takada, S. Matsunaga, K. Rissanen and M. Fujita, *Nature*, 2013, **495**, 461–6.

54 Y. Inokuma, M. Kawano and M. Fujita, *Nat. Chem.*, 2011, **3**, 349–58.

55 T. Kawamichi, T. Haneda, M. Kawano and M. Fujita, *Nature*, 2009, **461**, 633–635.

56 G.-H. Ning, Y. Inokuma and M. Fujita, *Chem. Asian J.*, 2014, **9**, 466–8.

57 K. Ikemoto, Y. Inokuma, K. Rissanen and M. Fujita, *J. Am. Chem. Soc.*, 2014, **136**, 6892–5.

58 S. Yoshioka, Y. Inokuma, M. Hoshino, T. Sato and M. Fujita, *Chem Sci*, 2015, **6**, 3765–3768.

59 T. R. Ramadhar, S.-L. Zheng, Y.-S. Chen and J. Clardy, *Chem. Commun.*, 2015, **51**, 11252–5.

60 N. Zigon, M. Hoshino, S. Yoshioka, Y. Inokuma and M. Fujita, *Angew. Chem. Int. Ed.*, 2015, **54**, 9033–7.

61 E. Sanna, E. C. Escudero-Adán, A. Bauzá, P. Ballester, A. Frontera, C. Rotger and A. Costa, *Chem. Sci.*, 2015, **6**, 5466–5472.

62 W. M. Bloch, N. R. Champness and C. J. Doonan, *Angew. Chem. Int. Ed.*, 2015, **54**, 12860–7.

63 J. D. Evans, C. J. Sumby and C. J. Doonan, *Chem. Soc. Rev.*, 2014, **43**, 5933–51.

64 A. J. Blake, N. R. Champness, T. L. Easun, D. R. Allan, H. Nowell, M. W. George, J. Jia and X.-Z. Sun, *Nat. Chem.*, 2010, **2**, 688–94.

65 W. M. Bloch, A. Burgun, C. J. Coghlan, R. Lee, M. L. Coote, C. J. Doonan and C. J. Sumby, *Nat. Chem.*, 2014, **6**, 906–12.

66 T. L. Easun, J. Jia, T. J. Reade, X.-Z. Sun, E. S. Davies, A. J. Blake, M. W. George and N. R. Champness, *Chem. Sci.*, 2014, **5**, 539–544.

67 J. S. Anderson, A. T. Gallagher, J. A. Mason and T. D. Harris, *J. Am. Chem. Soc.*, 2014, **136**, 16489–92.

68 W. M. Bloch, A. Burgun, C. J. Doonan and C. J. Sumby, *Chem. Commun.*, 2015, **51**, 5486–9.

69 S. Furukawa, J. Reboul, S. Diring, K. Sumida and S. Kitagawa, *Chem. Soc. Rev.*, 2014, **43**, 5700–34.

70 P. Falcaro, R. Ricco, C. M. Doherty, K. Liang, A. J. Hill and M. J. Styles, *Chem. Soc. Rev.*, 2014, **43**, 5513–60.

71 D. Bradshaw, S. El-Hankari and L. Lupica-Spagnolo, *Chem. Soc. Rev.*, 2014, **43**, 5431–43.

72 M. Tu, S. Wannapaiboon and R. A. Fischer, *Inorg. Chem. Front.*, 2014, **1**, 442.

73 I. Stassen, M. Styles, G. Grenci, H. V. Gorp, W. Vanderlinden, S. D. Feyter, P. Falcaro, D. D. Vos, P. Vereecken and R. Ameloot, *Nat. Mater.*, 2015, **15**, 304–310.

74 T. Kiyonaga, M. Higuchi, T. Kajiwara, Y. Takashima, J. Duan, K. Nagashima and S. Kitagawa, *Chem. Commun.*, 2015, **51**, 2728–30.

75 T. Rodenas, I. Luz, G. Prieto, B. Seoane, H. Miro, A. Corma, F. Kapteijn, F. X. Llabrés i Xamena and J. Gascon, *Nat. Mater.*, 2014, **14**, 48–55.

76 A. Sabetghadam, B. Seoane, D. Keskin, N. Duim, T. Rodenas, S. Shahid, S. Sorribas, C. L. Guillouzer, G. Clet, C. Tellez, M. Daturi, J. Coronas, F. Kapteijn and J. Gascon, *Adv. Funct. Mater.*, 2016, DOI: 10.1039/C6TA02611G.

77 Y. Sakata, S. Furukawa, M. Kondo, K. Hirai, N. Horike, Y. Takashima, H. Uehara, N. Louvain, M. Meilikhov, T. Tsuruoka, S. Isoda, W. Kosaka, O. Sakata and S. Kitagawa, *Science*, 2013, **339**, 193–6.

78 C. Zhang, J. A. Gee, D. S. Sholl and R. P. Lively, *J. Phys. Chem. C*, 2014, **118**, 20727–20733.

79 C. Avci, J. Ariñez-Soriano, A. Carné-Sánchez, V. Guillerm, C. Carbonell, I. Imaz and D. Maspoch, *Angew. Chem. Int. Ed.*, 2015, **54**, 14417–21.

80 X. Xu, Z. Zhang and X. Wang, *Adv. Mater.*, 2015, **27**, 5365–71.

81 J. Huo, J. Aguilera-Sigalat, S. El-Hankari and D. Bradshaw, *Chem. Sci.*, 2015, **6**, 1938–1943.

82 G.-Y. Jeong, R. Ricco, K. Liang, J. Ludwig, J.-O. Kim, P. Falcaro and D.-P. Kim, *Chem. Mater.*, 2015, **27**, 7903–7909.

83 Y. Yin, R. M. Rioux, C. K. Erdonmez, S. Hughes, G. A. Somorjai and A. P. Alivisatos, *Science*, 2004, **304**, 711–4.

84 K. Hirai, J. Reboul, N. Morone, J. E. Heuser, S. Furukawa and S. Kitagawa, *J. Am. Chem. Soc.*, 2014, **136**, 14966–73.

85 M. Pang, A. J. Cairns, Y. Liu, Y. Belmabkhout, H. C. Zeng and M. Eddaoudi, *J. Am. Chem. Soc.*, 2013, **135**, 10234–10237.

86 S. Wannapaiboon, M. Tu, K. Sumida, K. Khaletskaya, S. Furukawa, S. Kitagawa and R. A. Fischer, *J. Mater. Chem. A*, 2015, **3**, 23385–23394.

87 E. Zanchetta, L. Malfatti, R. Ricco, M. J. Styles, F. Lisi, C. J. Coghlan, C. J. Doonan, A. J. Hill, G. Brusatin and P. Falcaro, *Chem. Mater.*, 2015, **27**, 690–699.

88 K. Liang, C. Carbonell, M. J. Styles, R. Ricco, J. Cui, J. J. Richardson, D. Maspoch, F. Caruso and P. Falcaro, *Adv. Mater.*, 2015, **27**, 7483–7483.

89 J. Reboul, S. Furukawa, N. Horike, M. Tsotsalas, K. Hirai, H. Uehara, M. Kondo, N. Louvain, O. Sakata and S. Kitagawa, *Nat. Mater.*, 2012, **11**, 717–23.

90 K. Okada, R. Ricco, Y. Tokudome, M. J. Styles, A. J. Hill, M. Takahashi and P. Falcaro, *Adv. Funct. Mater.*, 2014, **24**, 1969–1977.

91 I. Stassen, N. Campagnol, J. Fransaer, P. Vereecken, D. De Vos and R. Ameloot, *CrystEngComm*, 2013, **15**, 9308.

92 N. Moitra, S. Fukumoto, J. Reboul, K. Sumida, Y. Zhu, K. Nakanishi, S. Furukawa, S. Kitagawa and K. Kanamori, *Chem. Commun.*, 2015, **51**, 3511–4.

93 K. Sumida, N. Moitra, J. Reboul, S. Fukumoto, K. Nakanishi, K. Kanamori, S. Furukawa and S. Kitagawa, *Chem. Sci.*, 2015, **6**, 5938–5946.

94 Z. Zhang, H. T. H. Nguyen, S. A. Miller and S. M. Cohen, *Angew. Chem. Int. Ed.*, 2015, **54**, 6152–7.

95 Y. Zhang, X. Feng, H. Li, Y. Chen, J. Zhao, S. Wang, L. Wang and B. Wang, *Angew. Chem. Int. Ed.*, 2015, **54**, 4259–63.

96 M. S. Denny and S. M. Cohen, *Angew. Chem. Int. Ed.*, 2015, **54**, 9029–32.

97 S. Sakaida, K. Otsubo, O. Sakata, C. Song, A. Fujiwara, M. Takata and H. Kitagawa, *Nat. Chem.*, 2016, **8**, 377–383.

98 Y. Wu, F. Li, Y. Xu, W. Zhu, C. Tao, J. Cui and G. Li, *Chem. Commun.*, 2011, **47**, 10094.

99 F. M. Hinterholzinger, A. Ranft, J. M. Feckl, B. Rühle, T. Bein and B. V. Lotsch, *J. Mater. Chem.*, 2012, **22**, 10356.

100 A. Ranft, F. Niekiel, I. Pavlichenko, N. Stock and B. V. Lotsch, *Chem. Mater.*, 2015, **27**, 1961–1970.

101 Z. Hu, C. Tao, F. Wang, X. Zou and J. Wang, *J Mater Chem C*, 2015, **3**, 211–216.

CrystEngComm Accepted Manuscript